

AD-A042 800

AEROSPACE CORP EL SEGUNDO CALIF SPACE SCIENCES LAB F/G 4/1  
INDUCED PRECIPITATION OF INNER ZONE ELECTRONS. VOLUME I. OBSERV--ETC(U)  
JUL 77 A L VAMPOLA, G A KUCK F04701-76-C-0077  
UNCLASSIFIED TR-0077(2260-20)-11-VOL-1 SAMSO-TR-77-134-VOL-1 NL

| of |  
ADA042800



END  
DATE  
FILMED  
9-77  
DDC

AD A 042800

# Induced Precipitation of Inner Zone Electrons

## Volume I: Observations

Space Sciences Laboratory  
The Ivan A. Getting Laboratories  
The Aerospace Corporation  
El Segundo, Calif. 90245

and

Advanced Concepts Division  
Space and Missile Systems Organization  
Air Force Systems Command

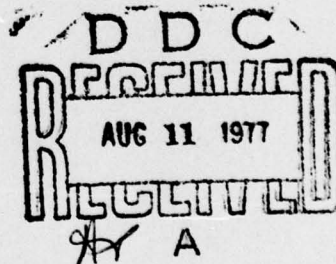
6 July 1977

Interim Report

APPROVED FOR PUBLIC RELEASE:  
DISTRIBUTION UNLIMITED

Prepared for

SPACE AND MISSILE SYSTEMS ORGANIZATION  
AIR FORCE SYSTEMS COMMAND  
Los Angeles Air Force Station  
P.O. Box 92960, Worldway Postal Center  
Los Angeles, Calif. 90009

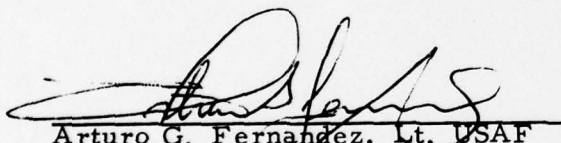


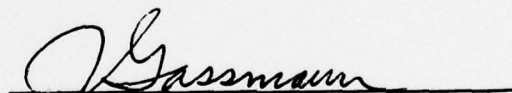
AD No. \_\_\_\_\_  
DDC FILE COPY

This interim report was submitted by The Aerospace Corporation, El Segundo, CA 90245, under Contract No. F04701-76-C-0077 with the Space and Missile Systems Organization, Deputy for Advanced Space Programs, P.O. Box 92960, Worldway Postal Center, Los Angeles, CA 90009. It was reviewed and approved for The Aerospace Corporation by G. A. Paulikas, Director, Space Sciences Laboratory. Lieutenant A. G. Fernandez, SAMSO/YAPT, was the project officer for Advanced Space Programs.

This report has been reviewed by the Information Office (OI) and is releasable to the National Technical Information Service (NTIS). At NTIS, it will be available to the general public, including foreign nations.

This technical report has been reviewed and is approved for publication. Publication of this report does not constitute Air Force approval of the report's findings or conclusions. It is published only for the exchange and stimulation of ideas.

  
Arturo G. Fernandez, Lt, USAF  
Project Officer

  
Joseph Gassmann, Major, USAF

FOR THE COMMANDER

  
LEONARD E. BALTZELL, Col, USAF, Asst.  
Deputy for Advanced Space Programs

UNCLASSIFIED

SECURITY CLASSIFICATION OF THIS PAGE (When Data Entered)

REPORT DOCUMENTATION PAGE		READ INSTRUCTIONS BEFORE COMPLETING FORM
1. REPORT NUMBER SAMSO-TR-77-134-61-1	2. GOVT ACCESSION NO.	3. RECIPIENT'S CATALOG NUMBER
4. TITLE (and Subtitle) INDUCED PRECIPITATION OF INNER ZONE ELECTRONS. Volume I: Observations	5. TYPE OF REPORT & PERIOD COVERED Interim report	
7. AUTHOR(s) Alfred L. Vampola (Aerospace) and George A. Kuck (SAMSO)	6. PERFORMING ORG. REPORT NUMBER TR-0077(2260-20)-11-Vol-1	
9. PERFORMING ORGANIZATION NAME AND ADDRESS The Aerospace Corporation El Segundo, Calif. 90245	8. CONTRACT OR GRANT NUMBER(s) F04701-76-C-0077	
11. CONTROLLING OFFICE NAME AND ADDRESS Space and Missile Systems Organization Air Force Systems Command Los Angeles, Calif. 90009	10. PROGRAM ELEMENT, PROJECT, TASK AREA & WORK UNIT NUMBERS	
14. MONITORING AGENCY NAME & ADDRESS (if different from Controlling Office)	12. REPORT DATE 11 6 July 1977	
	13. NUMBER OF PAGES 35 (236p)	
	15. SECURITY CLASS. (of this report) Unclassified	
15a. DECLASSIFICATION/DOWNGRADING SCHEDULE		
16. DISTRIBUTION STATEMENT (of this Report)  Approved for public release; distribution unlimited		
17. DISTRIBUTION STATEMENT (of the abstract entered in Block 20, if different from Report)		
18. SUPPLEMENTARY NOTES		
19. KEY WORDS (Continue on reverse side if necessary and identify by block number) Electron precipitation Wave-particle interactions Magnetospheric electrons		
20. ABSTRACT (Continue on reverse side if necessary and identify by block number) Narrow precipitation spikes of energetic electrons observed in the inner zone drift loss-cone during the 1968-1970 period by instrumentation on the OV1-14 and OV1-19 satellites are shown to have characteristics which are consistent with pitch-angle scattering produced through a resonant interaction with ground-based VLF transmissions. Analysis of the pitch-angle distributions indicates that for virtually all of the events, the electrons last interacted with the atmosphere in the vicinity of 55° to 62° East Longitude. The L-dependency of the spikes as a function of energy is consistent with scattering.		

DD FORM 1473  
(FACSIMILE)UNCLASSIFIED  
SECURITY CLASSIFICATION OF THIS PAGE (When Data Entered)

407512

UNCLASSIFIED

SECURITY CLASSIFICATION OF THIS PAGE(When Data Entered)

19. KEY WORDS (Continued)

20. ABSTRACT (Continued)

→ by a monochromatic wave. The presumption is that UMS, located at 44<sup>8</sup>E. and operating at a frequency of 16.2 kHz during this period, was responsible for these precipitation events. deg

ACCESSION for	
NTIS	White Section <input checked="" type="checkbox"/>
DDC	Buff Section <input type="checkbox"/>
UNANNOUNCED	<input type="checkbox"/>
JUSTIFICATION	
BY	
DISTRIBUTION/AVAILABILITY CODES	
Dist.	AVAIL. AND OF SPECIAL
A	

UNCLASSIFIED

SECURITY CLASSIFICATION OF THIS PAGE(When Data Entered)

## PREFACE

The authors wish to express their gratitude to Dr. Bruce Edgar for the ray-tracing calculations and to both Dr. Edgar and Dr. H. C. Koons for many fruitful discussions.

## CONTENTS

PREFACE .....	1
INTRODUCTION .....	5
INSTRUMENTATION .....	7
OBSERVATIONS .....	9
DISCUSSION .....	25
SUMMARY .....	31
REFERENCES .....	33

## FIGURES

1.	Energy spectra obtained by magnetic electron spectrometers on the OV1-14 satellite in 1968 in the drift loss-cone near $L = 1.68$ . . . . .	10
2.	Flux vs. time plots of data similar to those which produced the narrow energy distributions of Figure 1 . . . . .	11
3.	Data similar to those of Figure 2, but obtained by the OV1-19 satellite in 1969 . . . . .	12
4.	Schematic presentation of the drift loss-cone and the local bounce loss-cone as a function of East Longitude for $L = 1.75$ . . . . .	14
5.	Scatter plot of precipitation events observed by the OV1-19 as a function of East Longitude and time . . . . .	16
6.	A comparison of pitch-angle data from one event with the instrumental response to a hypothetical distribution which is isotropic between $60^\circ$ and $90^\circ$ and zero elsewhere . . . . .	18
7.	A plot of the equatorial pitch-angle of the observed local loss-cone vs. $L$ for the data of Figure 3 . . . . .	20
8.	A mapping of observed precipitation events back to their presumed origin using the method outlined in the text . . . . .	22
9.	$L$ dependence of the location of the peak at each energy for the events of Figure 8 . . . . .	23

## INTRODUCTION

The possibility of interactions between very-low-frequency electromagnetic waves and energetic electrons in the earth's magnetosphere has long been recognized. Dowden (1962) proposed that whistlers could be generated through a Doppler-shifted resonance with single electrons or electron bunches near the equator. Brice (1963) outlined a method for such an interaction with a general population of energetic electrons, since the required electron packet was an improbable initial condition. Brice also pointed out that this interaction, a cyclotron or transverse resonance, would result in the lowering of the pitch-angle of the electrons. Helliwell (1967) later generalized this result to permit explanation of rising tones through off-equatorial interaction regions.

A number of observations of naturally occurring VLF waves, generally lightning-generated whistlers or plasmopause hiss, have been reported as being correlated with electron precipitation. Rosenberg et al. (1971) and Foster and Rosenberg (1976), for instance, report correlations between VLF waves and x-rays observed by balloon-borne detectors. The actual particles have also been observed on satellites. Holzer et al. (1974) presented correlations between chorus observed near the outer edge of the stable trapping region and precipitation of  $>45$  keV electrons on OGO 6.

Attempts have been made to study propagation and amplification of VLF waves through generation and radiation of test signals from various places. A significant effort has centered around the Siple Station, Antarctica, transmissions and receptions at Roberval, Canada (Helliwell and Katsufakis, 1974). These efforts have led to significant results, but up to now no one has reported direct evidence (i. e., particles or x-rays) of actual pitch-angle

scattering of the electrons in an interaction with the waves. A second major effort of this type, which involved VLF transmissions from Alaska (see Koons et al., 1976), also appeared to produce no observable electron precipitation. In this latter project, some evidence of proton precipitation correlated with transmissions was observed (Koons, 1975), although it is unclear how protons could be affected by the waves themselves. Bell (1976) has proposed generation of ULF waves from VLF waves through an intermediate interaction with energetic electrons. The periodicity in amplification of VLF signals reported by Helliwell and Katsufakis (1974) might be an indication that the Bell suggestion is valid. No ground station magnetic field data were available to determine whether the modulated amplification was accompanied by ULF waves. If such waves are generated, they might be responsible for proton precipitation, if it occurs.

Other strong coherent sources of VLF waves are available and are routinely operating, although for the purposes of communication and navigation. No direct observation of particle precipitation due to these sources has been reported previously, although there is some evidence of enhanced E-region ionization resulting from high power HF transmissions (Wright, 1975). A possibility advanced by Wright was the establishment of a duct with the high power HF transmission, natural generation of VLF waves within the duct, and resultant precipitation of energetic electrons to produce the enhanced E-layer ionization. In the present paper, we report the observation of recurrent energetic electron precipitation with a number of unique parameters which we feel positively identifies it as being caused by the Russian VLF communications station, UMS.

## INSTRUMENTATION

The data presented here were obtained by sets of  $180^\circ$  focussing magnetic spectrometers on two different satellites during the 1968-1970 time period. The bulk of the data was obtained from the OV1-19 (1969-25C) magnetic electron spectrometers which have been discussed previously (Vampola, 1971). But the initial, and in some ways the best, observations were made by a pair of magnetic spectrometers flown on the OV1-14 (1968-26B) during April, 1968. The OV1-14 was a U.S. Air Force Office of Aerospace Research satellite launched into a  $100^\circ$  inclination elliptical orbit on April 6, 1968. Apogee and perigee were 9970 km and 550 km, respectively. The vehicle was spin-stabilized at about 10 RPM with the spin also being used to provide a scanning function for the scientific payload. An on-board magnetometer was used to obtain magnetic aspect for the particle instrumentation. Several days after launch, a failure in the spacecraft power system battery charging circuit caused overcharging and rupture of the battery, which resulted in premature termination of the mission. An on-board tape recorder stored up to four hours of data; seven tape dumps were achieved over a four-day period prior to termination of the mission.

The magnetic spectrometers on the OV1-14 were similar to others previously (and since) flown on other Air Force satellites. One was identical to the low energy unit on OV1-19 except for the magnetic field (380 gauss on the OV1-14) and the acceptance angle of the aperture. The other unit was the OV3-3 (1966-70A) backup instrument (Vampola, 1969) with a modified collimator. The field in this instrument was 1790 gauss. Each instrument contained a background detector to measure bremsstrahlung and penetrating particle responses. Table 1 gives the center energies and geometric-energy factors for the channels in both units.

TABLE 1

Channel	Low Energy Spectrometer		High Energy Spectrometer	
	Center Energy (MeV)	Geometric-Energy Factor (cm <sup>2</sup> -ster-keV)	Center Energy (MeV)	Geometric-Energy Factor (cm <sup>2</sup> -ster-keV)
1	.035	1.42	.531	15.8
2	.062	1.60	.809	14.9
3	.095	1.70	1.10	13.7
4	.132	1.75	1.40	12.6
5	.174	1.72	1.70	11.6
6	.219	1.63	2.00	10.3
7	.267	1.53	2.30	9.18
8	.318	1.43	2.60	8.29

## OBSERVATIONS

The time period of the OV1-14 data was the recovery period following a moderate magnetic storm on April 5, 1968. Highly monoenergetic precipitation spikes were seen in the electron distributions over a narrow range of L values for all low altitude passes over central and western Asia. Examples of these spikes are shown in Figure 1. The highly monoenergetic nature of these distributions suggested a resonant interaction with a monochromatic wave. The total precipitation event, in each instance, extended over about .15 L, but the observable flux enhancements at a given energy were much narrower. Fig. 2 illustrates the relationship of precipitated flux versus L at fixed energies and also the dispersion in L as a function of energy for the flux peak. The relatively high spin rate coupled with a long time constant for count rate meters at low count rates seriously degraded the accuracy with which pitch-angle distributions could be determined. The limited amount of data available from the OV1-14 satellite precluded a definitive study of the mechanism involved in this phenomenon although our original conjectures appear to be correct.

Recently, a large amount of data from the OV1-19 became available for analysis. Because of a low efficiency factor in the lowest energy channel and an early in-flight failure of the detector in the next lowest energy channel, the OV1-19 data set is not ideal for a complete study of the energy dependence of these precipitations. However, since it is an extensive data set, a search was made for events of the type seen in the OV1-14 data set. Figure 3 is a typical example of the same phenomenon as observed by the OV1-19 instrumentation. Note that the same characteristics are present: narrow distribution in L at any given energy; decreasing L location with increasing energy; L value between about 1.6 and 1.85.

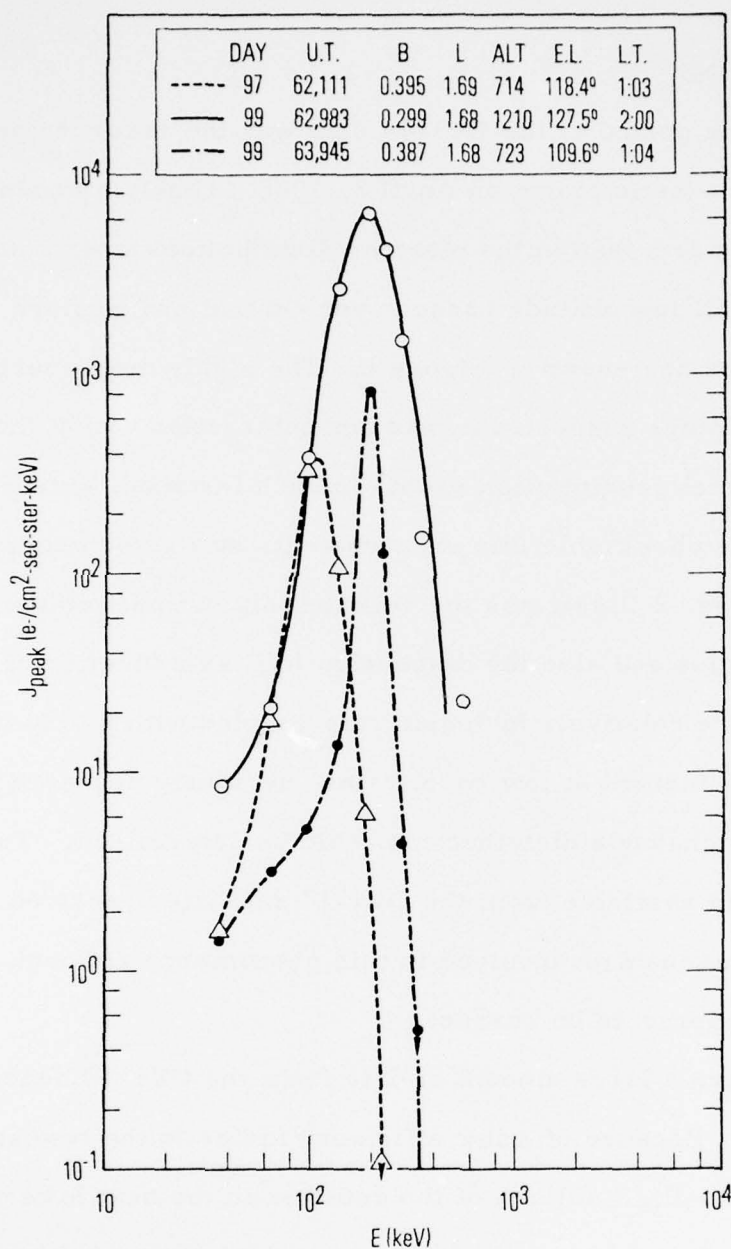


Figure 1 Energy spectra obtained by magnetic electron spectrometers on the OV1-14 satellite in 1968 in the drift loss-cone near  $L = 1.68$ . The narrow energy distributions indicate a resonant interaction is responsible for their appearance in the loss-cone.

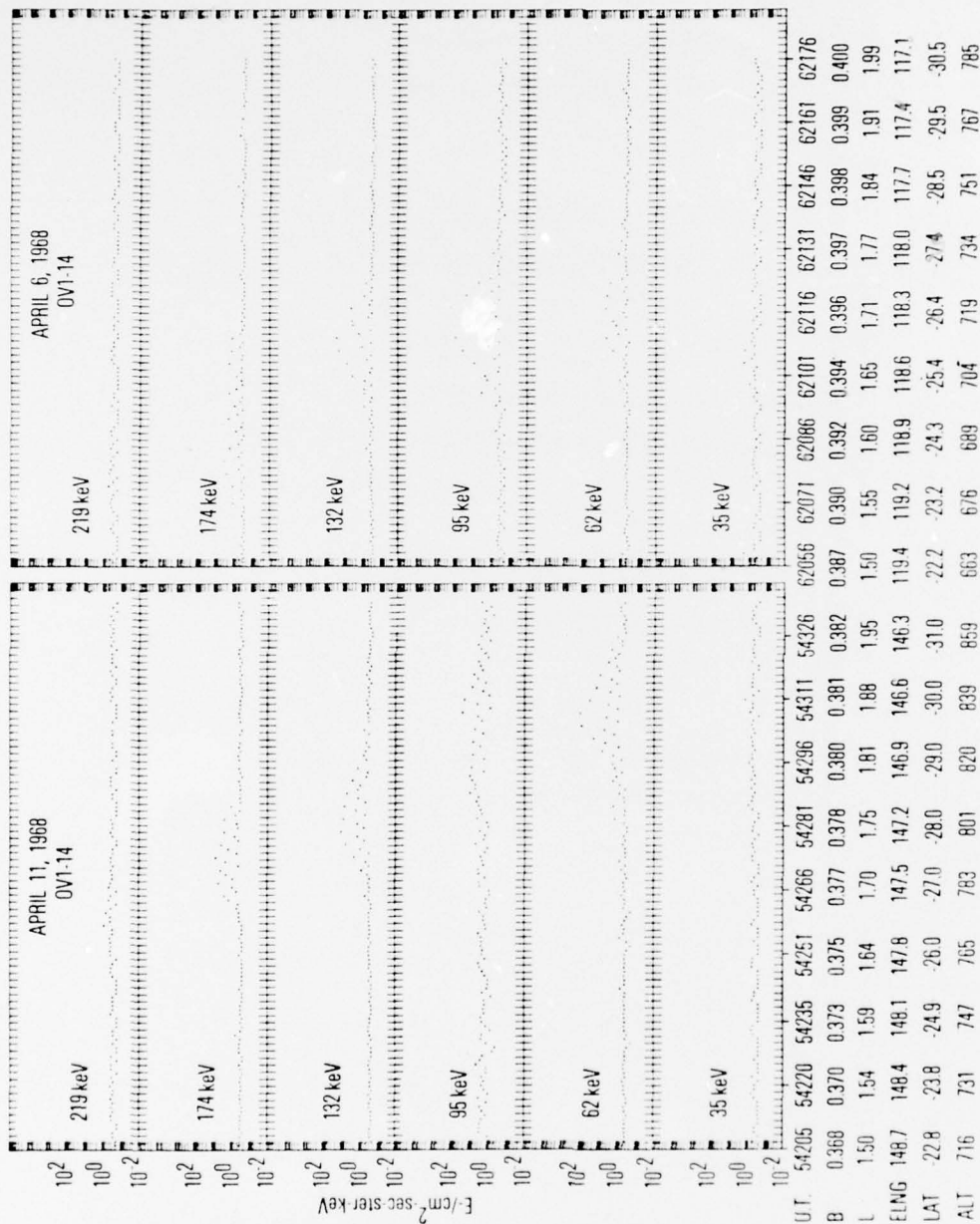


Figure 2 Flux vs. time plots of data similar to those which produced the narrow energy distributions of Figure 1. Note the monotonic variation in L of the peak of the precipitation distribution as a function of energy. The scatter in the data points is the result of pitch-angle sampling.

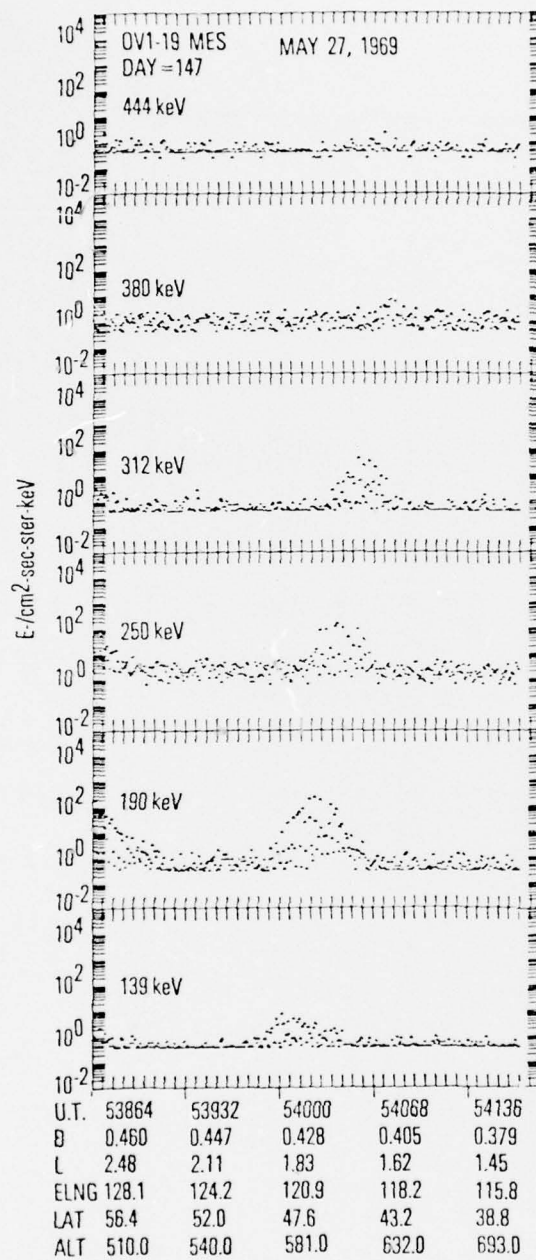


Figure 3 Data similar to those of Figure 2, but obtained by the OV1-19 satellite in 1969.

For the purposes of this investigation, use was made of the fact that electrons with small equatorial pitch-angles will be lost into the earth's atmosphere, as they drift eastward due to geomagnetic gradient effects, at a location determined by their pitch-angle and the local magnetospheric topography. A thorough discussion of this effect is available elsewhere (Roederer, 1970), but a brief discussion will be presented here since it is central to the identification of the source of these precipitation events. Figure 4 depicts the relationship between the equatorial pitch-angle of a particle on the  $L = 1.75$  shell and its destiny as a function of east longitude. For the purposes of Figure 4, it is assumed that a particle that has a local mirror point at or below 100 km will be immediately lost into the atmosphere; i. e., it is in the bounce loss-cone. A particle which has an equatorial pitch-angle between that of the local bounce loss-cone and the maximum bounce loss-cone (which in this case occurs at about  $330^\circ$  E. L.) is defined as being in the drift loss-cone, since at some point in its drift, it will encounter a 100 km mirror altitude and be lost into the atmosphere. Particles with equatorial pitch-angles greater than this maximum bounce loss-cone angle are considered stably trapped. By limiting observations to that particle population which is currently in the drift loss cone, one can identify particles that have been pitch-angle scattered during the immediately preceeding drift period (or a portion of it). To put it picturesquely, for the example in Figure 4, the geomagnetic configuration at  $330^\circ$  E. L. has wiped the slate clean for equatorial pitch-angles up to  $27.6^\circ$ . Any perturbation at any longitude which lowers the pitch-angle of a particle to below  $27.6^\circ$  will cause the particle to either be locally precipitated or to reside in the drift loss-cone until it encounters the atmosphere in its eastward drift.

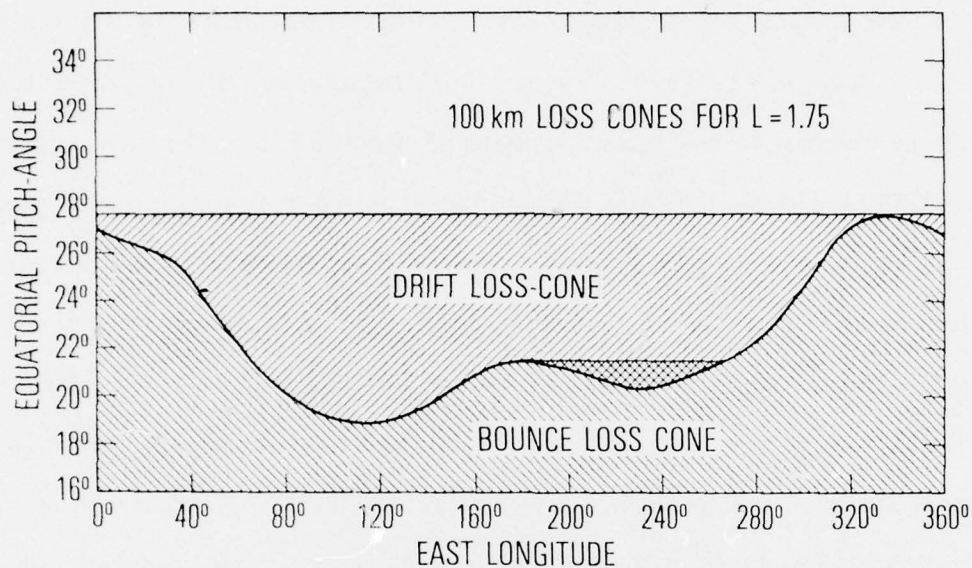


Figure 4 Schematic presentation of the drift loss-cone and the local bounce loss-cone as a function of East Longitude for  $L = 1.75$ . The bounce loss-cone is defined as the larger of either the north or south latitude 100 km bounce loss-cones. The cross-hatched portion between  $180^\circ$  and  $260^\circ$  East Longitude indicates a separate drift loss-cone determined by the magnetic field geometry at  $180^\circ$  E.L.

The portion of the OV1-19 data set that was available for this investigation was examined for the presence of events similar to those of Figs. 2 and 3, that is, of particles in the drift loss cone for the L interval 1.5 to 2.0. Of the eighty-eight periods of observation in this drift loss-cone region, thirty precipitation spikes were observed. The data set is shown graphically in Fig. 5 with time and east longitude as the parameters. Three symbols are used to depict: a) observation of a precipitation spike; b) no spike present although the spacecraft was in a location where others had been observed; c) no spike present but the spacecraft was below the drift shell defined by the atmosphere at  $50^{\circ}$  east longitude. (The actual minimum equatorial pitch-angle of this drift shell is a function of the L value.) The reason for the specification of the  $50^{\circ}$  E. drift shell will be made clear later. We can further divide the data set of Fig. 5, considering only those points which are defined in a) and b) above. We then find that of the 35 observation points prior to Day 262, 27 (or 77%) exhibited precipitation spikes. Of the remaining 22 points after Day 262, three (or 14%) had spikes. Since the OV1-19 orbit covered only a narrow range of local time (it was nearly sun-synchronous), possible correlations of the points of observation of spike events with local time could not be ascertained. There was no correlation with magnetic activity.

For the bigger events, sufficient intensity was available for accurate determination of the local pitch-angle distribution. The instrumentation contained count-rate meters which have sufficiently long time-constants at low count-rates that accurate determination of local loss-cone angles was not possible for most of the events. A peak count-rate of at least 200 counts/sec was required. For these larger events, one can construct an envelope

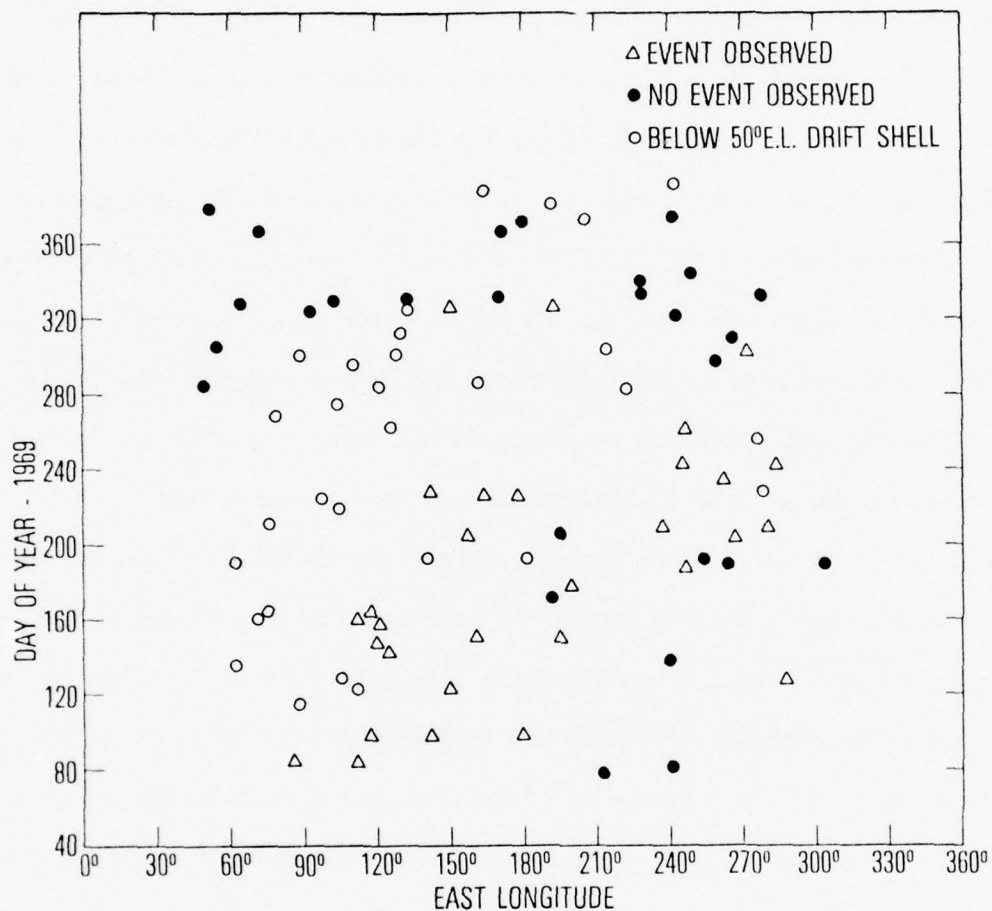


Figure 5 Scatter plot of precipitation events (and lack thereof) observed by the OV1-19 as a function of East Longitude and time. Circles indicate satellite passes in which the altitude was below the drift-loss-cone defined by the magnetic field geometry at  $50^\circ$  E. L. An abrupt change in the frequency of occurrence of events is evident about Day 260.

of the maxima in a spike at a given energy. Then, using  $L$  as a parameter, one can normalize all the data points in the event at that energy to the count-rate at the central  $L$  value, e. g.

$$N_{\text{normalized}} = N_{\text{observed}} \{ \exp[|L_{\text{center}} - L|/k] \}$$

where  $L$  is the instantaneous  $L$  value and  $k$  is derived from the envelope. In this manner, a fairly accurate, to about 2 degrees, determination of the local loss-cone angle could be made. The procedure also involved obtaining the convolution of the instrument response function with an assumed loss-cone angle. Figure 6 gives a typical result for an assumed loss-cone angle of  $60^\circ$  convoluted with the actual angular response function for the channel from which the data points of Fig. 6 were obtained. The data points are normalized data points. Note that the data must be almost two orders of magnitude above background before the time-constant effect in the rate-meters becomes negligible. For the data of Fig. 6, the maximum normalization factor was about 6.

Having obtained a reasonably accurate measurement of the local loss-cone angle, the equatorial pitch-angle of the observed loss-cone is easily determined using the local  $B$  value and assuming adiabatic motion. This angle then can be used to determine the location of the origin of the spike (see Luhmann and Vampola, 1977 for details). If one assumes that the size of the loss-cone is determined by the size of the local bounce loss-cone at the point of origin, one can trace back each event along its drift shell to the east longitude at which the instrumentally determined equatorial pitch-angle of the loss cone coincides with the local bounce loss cone

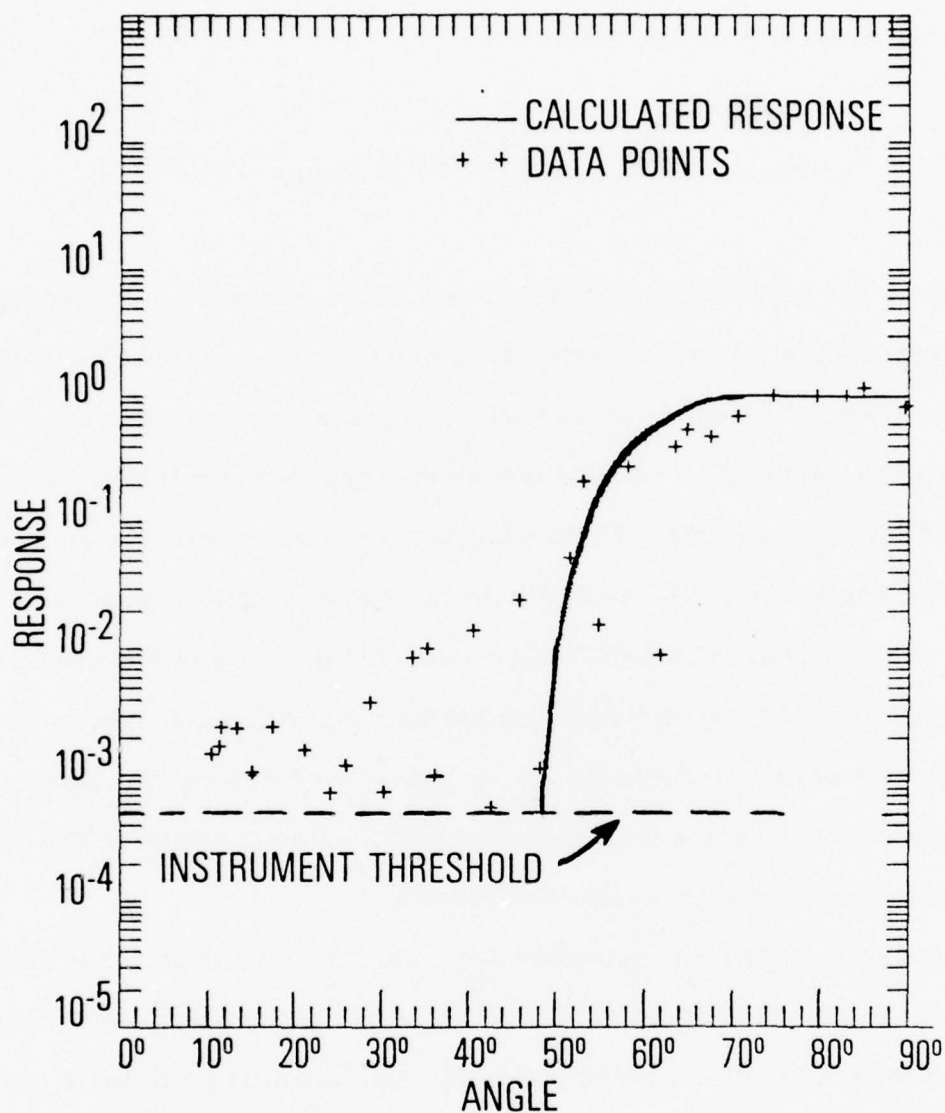


Figure 6 A comparison of pitch-angle data from one event with the instrumental response to a hypothetical distribution which is isotropic between  $60^\circ$  and  $90^\circ$  and zero elsewhere. The data points have been normalized. The "looping" which is apparent in the data at the low fluxes is due to the relatively long time-constants of the count-rate meter used in this instrument.

equatorial pitch-angle. We cannot show that the pitch-angle diffusion experienced by the particle after its initial perturbation is negligible, but we believe the data indicates that this is so.

Figure 7 presents the data of Figure 3 as an "L" vs "Equatorial Loss Cone Angle" plot. For this display, the procedure outlined above was used for each of the energies. For the 139 keV, 312 keV, and 380 keV channels, a local loss-cone angle of  $90^\circ$  was assumed, since the pitch-angle convolution procedure results were consistent with this value, although for the 312 keV channel  $87^\circ$  or  $88^\circ$  was also consistent. The other two channels had local loss-cones of  $84^\circ$  and  $85^\circ$ . These are significantly larger local loss-cones than were generally observed in the data because of the relatively low altitude of the observation. For most of the events, local loss-cones of  $50^\circ$  to  $75^\circ$  were observed. However, the error in determination of  $\alpha$ , the equatorial loss-cone angle, is considerably less for a large local loss-cone angle. For instance, at  $89^\circ$ , a  $1^\circ$  error in determination of the local loss-cone angle results in an error of only  $0.01^\circ$  in the equatorial loss-cone angle while at  $59^\circ$  local loss-cone angle, a  $1^\circ$  error results in an equatorial loss-cone angle error of almost  $0.5^\circ$ . A  $0.5^\circ$  equatorial angle variation translates to a  $5^\circ$  east longitude variation for values around  $60^\circ$  east longitude, as shown by Figure 4. For higher altitude data, the error would not be as extreme as this. Figure 7 also includes a curve showing the equatorial pitch-angle of particles which mirror at 100 km in the south and pass through the equatorial region at  $60^\circ$  east longitude. Typical mirror longitudes for these particles on these L-shells are  $66^\circ$  to  $68^\circ$  in the south and  $59^\circ$  in the north.

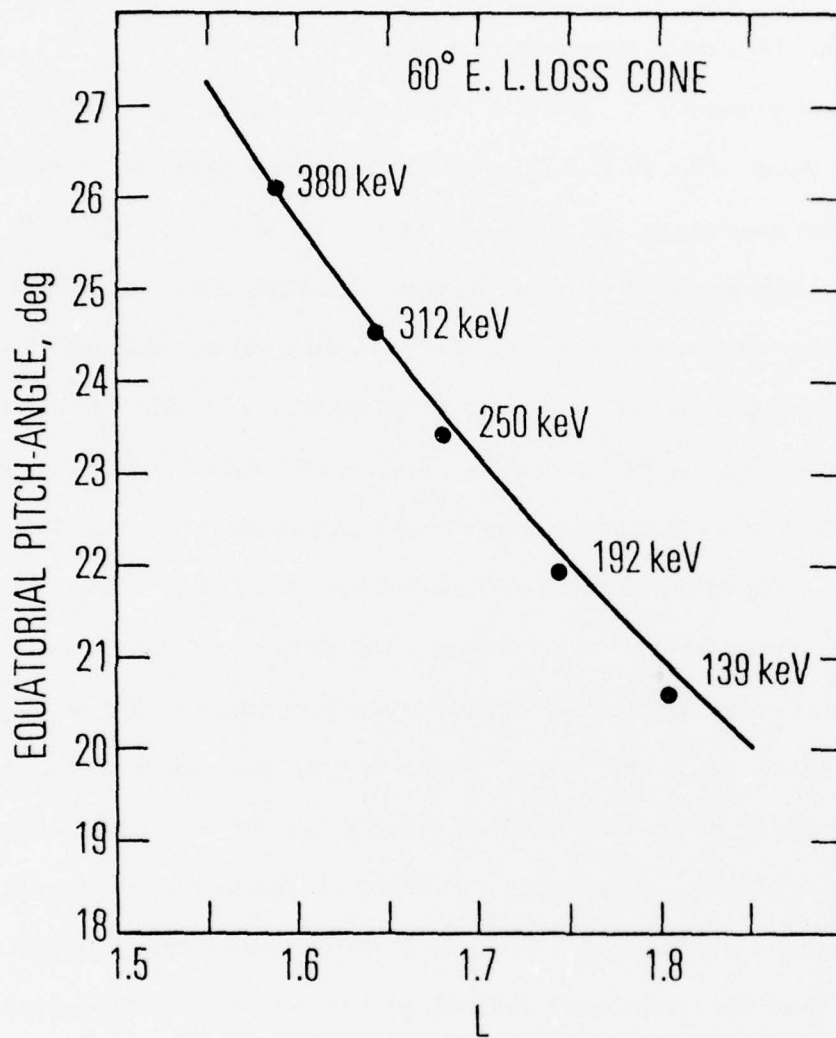


Figure 7 A plot of the equatorial pitch-angle of the observed local loss-cone vs.  $L$  for the data of Figure 3. The solid curve gives the equatorial pitch-angle as a function of  $L$  for particles which cross the magnetic equator at  $60^\circ$  East Longitude and mirror at 100 km in the southern hemisphere. Particles mirroring at 100 km in the northern hemisphere have smaller pitch-angles.

Figure 8 shows the 192 keV data for sixteen events mapped back from their points of observation to their points of origin as defined above. All but one of them map back to the region  $54^{\circ}$  to  $62^{\circ}$  E. with half of those being between  $54^{\circ}$  and  $56^{\circ}$ . An error in determination of the local loss cone angle of  $1^{\circ}$  leads to an error of about  $0.8^{\circ}$  in east longitude for these data.

For this mapping, we assumed the loss-cone angle was produced by a minimum altitude point in the southern hemisphere. We then determined the east longitude of the field-line which had the appropriate bounce-loss cone equatorial pitch-angle, and mapped back to the equatorial crossing along the field line. The field model used was the POGO (8/69) model (Cain and Sweeney, 1970).

The data of Figure 7 indicate that particles of various energies are being precipitated at the same longitude but not at the same L shell. The data of Figures 2 and 3 indicate both regularity and monotonicity in the distribution of the various energy peaks as a function of L. To investigate this possible correlation, the events used in Figure 8 to map back in longitude were also plotted on an ENERGY vs. L diagram, shown as Figure 9. For this plot, the L value of the peak intensity for each energy channel was used, with an accuracy of about  $\pm .01$  L. The energy assigned to each channel was the centroid of the energy response for a flat spectrum (which should be fairly well approximated at the peak of each precipitation spike, as shown by Figure 1). Calculations of the expected resonant energy at the equator as a function of L for a 16.2 kHz wave (non-ducted) for two typical cold electron densities are also shown. These calculations were done by the method of ray-tracing using a diffusive equilibrium

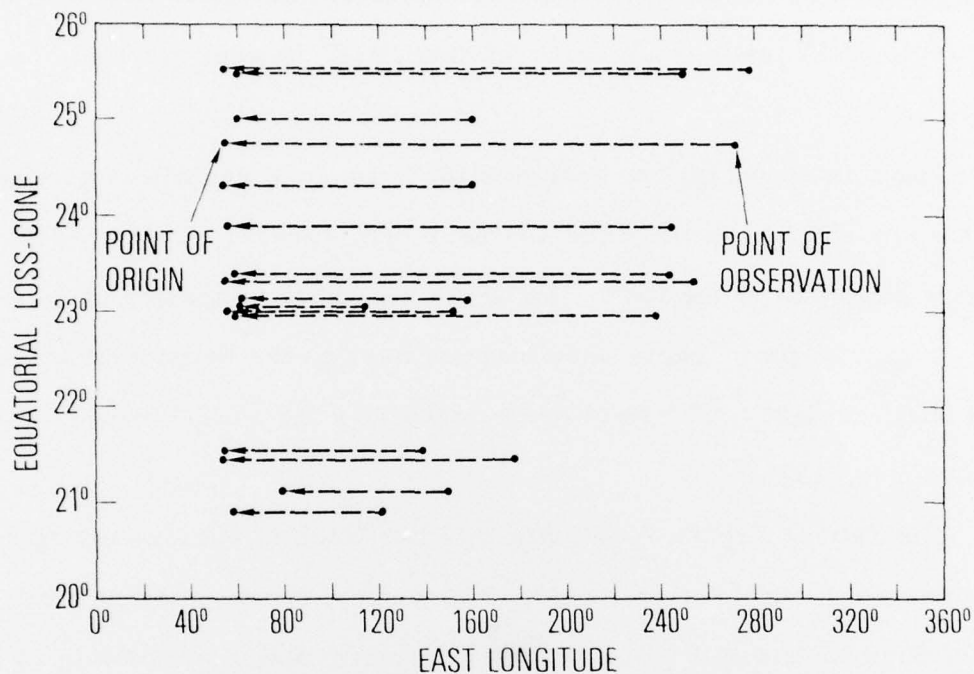


Figure 8 A mapping of observed precipitation events back to their presumed origin using the method outlined in the text. These are all OV1-19 data from the 192 keV channel. The large variation in equatorial loss-cone angle mapping back to approximately the same East Longitude is due to a relatively large variation in L from event to event for the peak in precipitation.

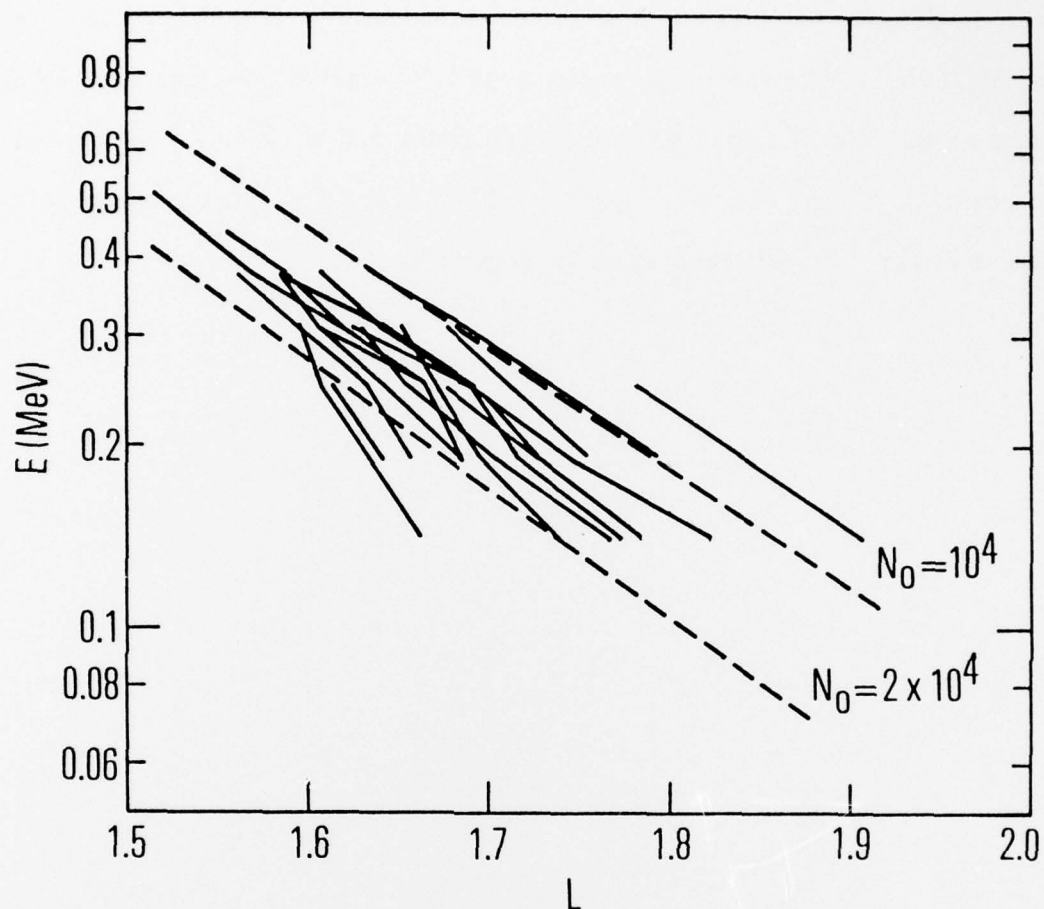


Figure 9 L dependence of the location of the peak at each energy for the events of Figure 8. The dashed lines are the expected resonant energies at the equator for a 16.2 kHz wave for two typical diffusive-equilibrium electron density models.  $N_0$  refers to the base level electron density at 1000 km.

model for the magnetospheric electron density model of Angerami and Thomas (1964). The model parameters consisted of a constant base electron density at 1000 km and  $H^+/O^+$  ion mixture of 90%/10% at a temperature of  $1600^{\circ}K$ . At 1000 km for an L of 1.97 during the spring of 1965, Brace et al. (1967) reported variations from  $1.3 \times 10^4 \text{ cm}^{-3}$  at a local time of 1300 hrs to  $2.5 \times 10^4 \text{ cm}^{-3}$  at 0100 hrs LT. These numbers are quite similar to the values used in Figure 9.

## DISCUSSION

The data of Figures 1-3 indicate a narrow-band resonance is involved in the precipitation of these electrons in the inner zone. While the possibility of such a narrow resonance being caused by a natural instability cannot be ruled out on fundamental grounds, no such narrow resonance has been observed in wave data from satellites. (We are not considering the various cold proton and electron gyroresonances as possibilities here; nor are we going to consider anomalous amplification of VLF signals as being a natural source.)

If one makes the assumption that the precipitations are due to artificially generated VLF waves, the first task is to identify the source of those waves. The mapping procedure which resulted in Figure 8 indicates that the source of all the precipitations examined was west of  $80^{\circ}$  E. L. and, for all but one event, was west of  $61^{\circ}$  E. L. Figure 4 indicates that by the time the electron population has drifted from  $330^{\circ}$  E. to  $60^{\circ}$  E., the  $L = 1.75$  bounce loss-cone angle decreases from about  $28^{\circ}$  to  $22^{\circ}$  (equatorial pitch-angle). The highly asymmetric pitch-angle distribution created by the South Atlantic Anomaly seems to be a prime candidate for a Kennel-Petschek (1966) instability. The empty portion of the drift loss cone would serve as an excellent background against which to see such an instability precipitate a portion of the asymmetric distribution. However, we can rule that out as a source for these precipitations on a number of grounds.

First of all, such a process would not be energy selective, since the asymmetric distribution occurs at all energies. Figure 1 shows our

process IS energy selective. Second, the process would not be highly selective in L. Figures 2 and 3 again show that ours is. Third, the data of Figure 5 show an abrupt change in the frequency of occurrence of these events after Day 260. This is also incompatible with a K-P instability as the source. Finally, there was no correlation between these events and magnetic activity. Since the low energy particle population at these L values is enhanced during and following major magnetic storms (Bostrom et al., 1970; Vampola, 1972), the asymmetry east of the anomaly is greater following such storms than before. Large storms occurred around Day 135 and Day 270, but these had no effect on the frequency of observance of events or on the amount of precipitation occurring in a single event.

The source of these precipitation events rotates with the earth, as shown by the fact that 15 of the 16 events mapped in Figure 8 originated between  $54^{\circ}$  and  $62^{\circ}$  E. Figure 7, for instance, shows that all energies, although at different L values and with different equatorial loss cone angles, last interacted strongly with the atmosphere at about  $60^{\circ}$  E. Since the equatorial loss-cone angle is decreasing with eastward drift at that location, we can assume that all energies were precipitated there. Of course, particles could also have been precipitated at longitudes farther west, but those particles would have a larger loss-cone angle. The fact that events observed half-way around the world to the east from where they last interacted with the atmosphere show similar loss-cone angles indicates that the pitch-angle diffusion due to non-atmospheric causes is very weak. Otherwise, there would be a tendency for events observed farther east to have smaller loss-cones. The slightly smaller loss-cones observed

at lower energy in Figure 7 may be due either to slow pitch-angle diffusion which is more effective at low energy or may be indicative that the precipitation mechanism continues to operate farther to the east for lower energy particles. A precipitation cause which rotates with the earth is strongly suggestive of a ground-based VLF transmitter. The radiation pattern from the transmitter diminishes in intensity with distance and hence might be effective only on the lowest energy electrons at greater distances.

In the neighborhood of  $60^{\circ}$  E., there were at least two VLF stations: a relatively low power transmitter at Algazy, USSR, at  $77^{\circ} 11'$  E.,  $43^{\circ} 50'$  N. that operated at 16.1 kHz (Aksenov et al., 1970), and a high power (315 kw) transmitter at Gorky, USSR, at  $44^{\circ}$  E.,  $46.2^{\circ}$  N., that has operated as UMS on 17.1 kHz and as RPS at 16.2 kHz (Watt, 1967; Amon and Dowden, 1976).

The plot of the energy dependence of the location of the peaks as a function of L shown in Figure 9 indicates that a single frequency with a single electron density for the unducted calculations gives reasonable agreement. The slope is similar to that reported by Imhof et al. (1974a) for L-dependent peaks in 1971-1972. Frequencies of 8 to 15 kHz were indicated as being compatible with those observations. For those data, Imhof et al. concluded that the peaked spectra precipitations occurred preferentially in the early dawn hours. In our data, we consider the variations as being due to a local-time variation in the electron density with a constant perturbing frequency rather than a variable perturbing frequency. Detailed wave-tracing studies on this data set are in progress.

The sudden change in the frequency of occurrence of these precipitation spikes which occurred after Day 260 is currently unexplained. If a transmitter at Gorky is assumed, precipitation spikes should be observable whenever the satellite is in the drift loss-cone above an altitude determined by the bounce loss-cone at the point farthest to the east that the precipitation mechanism is effective. Since most of the events mapped back to  $55^{\circ}$ - $60^{\circ}$ , a conservative limit of  $50^{\circ}$  was set for the determination of the presence or absence of an event. Previous studies of triggered emissions indicate that a CW signal of about 125 msec is required to trigger the instability that leads to wave growth (and presumably particle pitch-angle scattering). If a single dash in a transmission from Gorky can produce precipitation to as far as  $60^{\circ}$  E.L., a region of tens of degrees in longitude presumably is filled with drift loss-cone electrons. Since the drift rate of these electrons is of the order of  $2^{\circ}$  per minute, it would take on the order of ten minutes for the effects of a single dash to drift through the plane of the satellite's orbit. Hence, relatively infrequent communications transmissions would be sufficient to produce effectively steady-state precipitation effects. However, it is known that the transmissions from Gorky were not always CW. Frequency Shift Keying, which was also used, probably would not produce precipitation. The duration of transmission of a given frequency in FSK is probably too short to produce triggered emissions. An additional piece of evidence of the efficacy of producing particle precipitation by FSK is given indirectly by Bullough et al. (1976) in which GBR signals at 16 kHz received aboard Ariel III were characteristically an order of magnitude stronger in CW than in FSK. Hence, the change in frequency of observation of precipitation events which occurred

during 1969 may reflect a change in the operating mode of the transmitter. A complete study of this effect would require a detailed operating log from the transmitter. Such a log would permit quantitative analysis of the effects, including the drift periods and the local pitch-angle. It would also permit identification of the area over which the transmissions were able to produce precipitation.

In addition to the events included in this study, other precipitation spikes with different characteristics were also observed. Several were "multiple peak" events, with two or more peaks, at different L, for each energy. Possible explanations are: a) multiple transmitting frequencies, perhaps as much as 10 minutes apart in time; b) transmitters at different sites (and therefore at different local times, providing different base electron densities); c) a non-uniform ionosphere. Also, a single "ducted" event was observed in which all channels up to and including the 531 keV channel were observing precipitation at the same L shell. The observed loss-cone coincided with the local loss-cone. Hence, either the duct was local (at  $288^{\circ}$  E.L.) or could have been located anywhere east of about  $40^{\circ}$  E.L. All these events are being analyzed.

The practical and geophysical implications of artificially induced precipitation of radiation belt electrons are far-reaching. Bullough et al. (1976) suggested that harmonics of the extensive 50-60 Hz power grids in North American and Europe are effective in precipitating electrons and may be responsible, in part, for the existence of the slot at  $2 < L < 3$ . Imhof et al. (1974b) observed what they called "resonance precipitation" of electrons in the slot region which was consistent with plasmaspheric

hiss observed in the slot. The hiss may be the result of amplification of high order harmonics of power grids. If other man-made sources of ELF/VLF are effective in the precipitation of electrons, and there are a number of very powerful transmitters around the world used for navigation and communications, the possibility exists that the gross morphology of the radiation belts may be the result of man's transmissions. Perhaps weak pitch-angle diffusion observed in the outer belt (e.g., Williams et al., 1968) is entirely due to such emissions. A significant and unambiguous confirmation that this mechanism is operative could be made, of course, by turning off all sources of man-made ELF/VLF/LF, including power grids. A realistic method would be to produce time-averaged intensity plots of particles in the bounce loss-cone as a function of longitude and latitude. If only a small number of discrete sources of precipitation exist, they would be readily observable. The effect of the power grids over North America should be discernable if sufficient resolution in both energy and latitude is available.

## SUMMARY

Highly monoenergetic spikes of energetic electrons were observed in the drift loss-cone at L-values of 1.6 to 1.85 during the 1968-1970 period by magnetic spectrometers on the OV1-14 and OV1-19 satellites. Using the locally observed loss-cone angles, these spikes were determined to have last interacted with the atmosphere in the region of  $55^{\circ}$  to  $62^{\circ}$  East Longitude, indicating that the cause of the precipitation was corotating with the earth. The energy dependence of the position in L of the precipitation was shown to agree with the predicted interaction region for unducted waves with a frequency similar to the Russian communications VLF transmitter which was located near the observed source of the precipitations. Although the geomagnetic topography over eastern Europe makes this an ideal location for observing effects of VLF transmissions on the trapped particle population, since in this region the South Atlantic Anomaly has produced a large empty loss-cone, it should be possible to see similar effects from other powerful VLF transmitters by carefully studying the local bounce loss-cone on a worldwide basis. The identification of direct precipitation of electrons by ground-based VLF stations adds further support to the idea advanced by Bullough et al. (1976) that significant features in the electron belts may be due to man-made transmissions.

# REFERENCES

- Aksenov, V. I., B. A. Dubinskii, L. A. Zhekulin, Z. Ya. Kiseleva, I. V. Lishin, V. A. Makarov and L. N. Mikhailov, Investigation of Transmission of Ultralong Radio Waves through the Earth's Ionosphere: Preliminary results from the Cosmos 142 satellite, Cosmic Research, 8, 527, 1970.
- Amon, L. E. S. and R. L. Dowden, VLF stations detected at Dunedin, 1976 (Unpublished report, University of Otago, Dunedin, New Zealand).
- Angerami, J. J. and J. O. Thomas, Studies of Planetary Atmospheres, 1, The distribution of electrons and ions in the earth's exosphere, J. Geophys. Res., 69, 467, 1964.
- Bell, T. F., ULF Wave generation through particle precipitation induced by VLF transmitters, J. Geophys. Res., 81, 3316, 1976.
- Bostrom, C. O., D. S. Beall and J. C. Armstrong, Time history of the inner radiation zone, October 1963 to December 1968, J. Geophys. Res., 75, 1246, 1970.
- Erace, L. H., B. M. Reddy and H. G. Mayr, Global behavior of the ionosphere at 1000 km altitude, J. Geophys. Res., 72, 265, 1967.
- Brice, N., An explanation of triggered Very-Low-Frequency emissions, J. Geophys. Res., 68, 4626, 1963.
- Bullough, K., A. R. L. Tatnall and M. Denby, Man-made ELF/VLF emissions and the radiation belts, Nature, 260, 401, 1976.
- Cain, J. C., and R. E. Sweeney, Magnetic field mapping of the inner magnetosphere, J. Geophys. Res., 75, 4360, 1970.
- Dowden, R. L., Doppler-shifted cyclotron radiation from electrons: A theory of very low frequency emissions from the exosphere, J. Geophys. Res., 67, 1745, 1962.
- Foster, J. C. and T. J. Rosenberg, Electron precipitation and VLF emissions associated with cyclotron resonance interactions near the plasmapause, J. Geophys. Res., 81, 2183, 1976.
- Helliwell, R. A., and J. P. Katsufakis, VLF wave injection into the magnetosphere from Siple Station, Antarctica, J. Geophys. Res., 79, 2511, 1974.
- Helliwell, R. A., A theory of discrete VLF emissions from the magnetosphere, J. Geophys. Res., 72, 4773, 1967.
- Helliwell, R. A., J. P. Katsufakis, M. Trimpf, and N. Brice, Artificially stimulated very-low-frequency radiation from the ionosphere, J. Geophys. Res., 69, 2391, 1964.
- Holzer, R. E., T. A. Farley, R. K. Burton, and M. C. Chapman, A correlated study of ELF waves and electron precipitation on OGO 6, J. Geophys. Res., 79, 1007, 1974.

- Imhof, W. L., E. F. Gaines and J. B. Reagan, L Dependent peaks in the energy spectra of electrons precipitating from the inner belt, in Magnetospheric Physics, B. M. McCormac, ed., D. Reidel, Dordrecht-Holland, 1974a.
- Imhof, W. L., E. E. Gaines and J. B. Reagan, Evidence for the resonance precipitation of energetic electrons from the slot region of the radiation belts, *J. Geophys. Res.*, 79, 3141, 1974b.
- Kennel, C. F. and H. E. Petschek, Limit on stably trapped particles, *J. Geophys. Res.*, 71, 1, 1966.
- Koons, H. C., Proton precipitation by a whistler-mode wave from a VLF transmitter, *Geophys. Res. Lett.*, 2, 281, 1975.
- Koons, H. C., M. H. Dazey, R. L. Dowden, and L. E. S. Amon, A controlled VLF phase reversal experiment in the magnetosphere, *J. Geophys. Res.*, 81, 5536, 1976.
- Luhmann, J. G., and A. L. Vampola, Effects of localized sources on quiet-time plasmasphere electron precipitation, *J. Geophys. Res.*, 82, 1977.
- Roederer, J. G., Dynamics of geomagnetically trapped radiation, Springer-Verlag, New York, 1970.
- Rosenberg, T. J., R. A. Helliwell, and J. P. Katsufakis, Electron precipitation associated with discrete Very-Low-Frequency emissions, *J. Geophys. Res.*, 76, 8445, 1971.
- Vampola, A. L., Natural variations in the geomagnetically trapped electron population, in Proceedings of the National Symposium on Natural and Manmade Radiations in Space, E. A. Warman, ed., NASA TM X-2400, p. 539, 1972.
- Vampola, A. L., Access of solar electrons to closed field lines, *J. Geophys. Res.*, 76, 36, 1971.
- Vampola, A. L., Energetic electrons at latitudes above the outer zone cutoff, *J. Geophys. Res.*, 74, 1254, 1969.
- Watt, A. D., VLF Radio Engineering, Pergamon Press, Ltd., 1967.
- Williams, D. J., J. F. Arens and L. J. Lanzerotti, Observations of trapped electrons at Low and High altitude, *J. Geophys. Res.*, 73, 5673, 1968.
- Wright, J. W., Evidence for precipitation of energetic particles by ionospheric "Heating" transmissions, *J. Geophys. Res.*, 80, 4383, 1975.

### THE IVAN A. GETTING LABORATORIES

The Laboratory Operations of The Aerospace Corporation is conducting experimental and theoretical investigations necessary for the evaluation and application of scientific advances to new military concepts and systems. Versatility and flexibility have been developed to a high degree by the laboratory personnel in dealing with the many problems encountered in the nation's rapidly developing space and missile systems. Expertise in the latest scientific developments is vital to the accomplishment of tasks related to these problems. The laboratories that contribute to this research are:

Aerophysics Laboratory: Launch and reentry aerodynamics, heat transfer, reentry physics, chemical kinetics, structural mechanics, *flight dynamics*, atmospheric pollution, and high-power gas lasers.

Chemistry and Physics Laboratory: Atmospheric reactions and atmospheric optics, chemical reactions in polluted atmospheres, chemical reactions of excited species in rocket plumes, chemical thermodynamics, plasma and laser-induced reactions, laser chemistry, propulsion chemistry, *space vacuum* and radiation effects on materials, lubrication and surface phenomena, photosensitive materials and sensors, high precision laser ranging, and the application of physics and chemistry to problems of law enforcement and biomedicine.

Electronics Research Laboratory: Electromagnetic theory, devices, and propagation phenomena, including plasma electromagnetics; quantum electronics, lasers, and electro-optics; communication sciences, applied electronics, semiconducting, superconducting, and crystal device physics, optical and acoustical imaging; atmospheric pollution; millimeter wave and far-infrared technology.

Materials Sciences Laboratory: Development of new materials; metal matrix composites and new forms of carbon; test and evaluation of graphite and ceramics in reentry; spacecraft materials and electronic components in nuclear weapons environment; application of fracture mechanics to stress corrosion and fatigue-induced fractures in structural metals.

Space Sciences Laboratory: Atmospheric and ionospheric physics, radiation from the atmosphere, density and composition of the atmosphere, aurorae and airglow; magnetospheric physics, cosmic rays, generation and propagation of plasma waves in the magnetosphere; solar physics, studies of solar magnetic fields; space astronomy, x-ray astronomy; the effects of nuclear explosions, magnetic storms, and solar activity on the earth's atmosphere, ionosphere, and magnetosphere; the effects of optical, electromagnetic, and particulate radiations in space on space systems.

THE AEROSPACE CORPORATION  
El Segundo, California